Southern Hemisphere In Situ Observations of OH, HO_2, ClO and BrO from the ER-2 Aircraft for the 1994 ASHOE Mission

Final Technical Report
NASA-Langley Agreement No. NAG-1-1609
April 11, 1994–April 10, 1995

Submitted to
National Aeronautics and Space Administration
from
The President and Fellows of Harvard College
c/o Office for Sponsored Research
Holyoke Center, Room 458
1350 Massachusetts Avenue
Cambridge, Massachusetts 02138

James G. Anderson, Principal Investigator
Department of Chemistry
Harvard University
12 Oxford Street
Cambridge, Massachusetts 02138

January 30, 1996

Note: Funding for this research was split between two grants from NASA Langley: NAG-1-1617 (for field research) and NAG-1-1609 (development/analysis work in support of the field mission). This report is submitted as the Final Technical Report for both grants.

The NASA Arctic Southern Hemisphere Ozone Experiment (ASHOE) campaign involved forty flights of the ER-2 from Ames Research Center, Moffett Field, CA; Barbers Point Naval Air Station, Hawaii; Nadi Field, Fiji; and Christchurch, New Zealand. The responsibility of the Harvard research team was the *in situ* observation of the radicals OH, HO_2, ClO and BrO, with corollary observations of ozone and water vapor. These radicals constitute the reactants in the rate limiting steps of the catalytic cycles that control the destruction rate of ozone in the lower stratosphere. The instruments performed very well throughout the course of the ER-2 flights for the ASHOE campaign. The data analysis is complete for that mission and the data have been submitted to the mission data network for open access by the scientific community. Key results prepared for publication are attached as appendices to this report.

A summary of the first order scientific conclusions that emerged from the research done under this grant are as follows:

1. For the first time, the concentration of the key hydrogen and halogen radicals OH, HO_2, ClO and BrO were determined on a global scale extending from the arctic circle to the antarctic circle, over the altitude domain of the ER-2. That domain extends from 15–20 km altitude, covering a critical part of the lower stratosphere.
2. Simultaneous, *in situ* measurements of the concentrations of OH, HO_2, ClO, BrO, NO and NO_2 demonstrate the predominance of odd-hydrogen and halogen free radical catalysis in determining the rate of removal of ozone in the lower stratosphere over the complete ASHOE mission. This extends to the global scale the "first look" data obtained during the NASA Stratospheric Photochemistry and Dynamics Experiment (SPADE), executed out of Ames Research Center in June 1993. This represents a major rearrangement of our understanding with respect to the hierarchy of dominant catalytic cycles controlling ozone loss in the lower stratosphere. For the past twenty

years, it has been assumed that nitrogen radicals dominate the destruction rate of ozone in the lower stratosphere.

3. Throughout the altitude and latitude range covered by ASHOE, it was determined that a single catalytic cycle, $HO_2 + O_3 \rightarrow OH + 2O_2$, accounted for one half of the total O_3 removal in this region of the atmosphere. Halogen radical catalytic cycles were found to account for one third of the ozone loss, and nitrogen radicals were found to account for 20% of the loss.
4. Simultaneous observations of the full complement of radicals, tracers, ozone, and water vapor during ASHOE demonstrated quantitatively the coupling that exists between the rate limiting radicals and other reactive species in the photochemical reaction network. Specifically, the concentrations of ClO and HO_2 are inversely correlated with the concentration of NO_x. This carries the implication that the NO_x effluent from the proposed High Speed Civil Transport may be less destructive to stratospheric ozone than had previously been thought. ASHOE brought this conclusion forward for the first time on a global basis.
5. The density of BrO was measured on a global scale during ASHOE in the lower stratosphere. It was found that bromine is responsible for 55–65% of the local rate of catalytic destruction of ozone by reactions involving bromine and chlorine. Normalizing calculated loss rates to total available inorganic bromine and chlorine explicitly demonstrates that bromine is 60–80 times more efficient than chlorine in removing ozone in the lower stratosphere. An inferred value of total inorganic bromine is in excellent agreement with measurements of their source species, organic bromine compounds in the troposphere.

Publications

1. Stimpfle, R. M., D. W. Kohn, P. O. Wennberg, R. C. Cohen, T. Hanisco, J. G. Anderson, R. J. Salawitch, J. W. Elkins, G. S. Dutton, M. Volk, R. S. Gao, D. W. Fahey, "Bromine in the lower stratosphere: *In situ* measurements of BrO from the NASA ER-2 aircraft," *Science*, submitted, January 1996.
2. Hanisco, T. F., P. O. Wennberg, R. C. Cohen, J. G. Anderson, D. W. Fahey, E. R. Keim, R. S. Gao, R. C. Wamsley, S. G. Donnelly, L. A. Del Negro, R. J. Salawitch, K. K. Kelly, and M. H. Proffitt, "*In situ* measurements of HO_x for super- and subsonic aircraft exhaust plumes," *Science*, in preparation, 1996.

3. Kohn, D. W., R. M. Stimpfle, P. O. Wennberg, T. F. Hanisco, and J. G. Anderson, "Constraints on sulfate aerosol reactions along back trajectories imposed by HO_x and ClO_x *in situ* measurements," *J. Geophys. Res.*, in preparation, 1996.

Submitted to Science, January 1996

Bromine Catalyzed Removal of Ozone: In Situ Measurements of BrO in the Lower Stratosphere

R. M. Stimpfle*, D. W. Kohn, P. O. Wennberg, R. C. Cohen, T. F. Hanisco, J. G. Anderson, R. J. Salawitch, J. W. Elkins, R. S. Gao, D. W. Fahey, M. H. Proffitt, M. Loewenstein and K. R. Chan

Abstract: Observations of the BrO radical in the lower stratosphere obtained simultaneously with measurements of short-lived hydrogen, nitrogen and chlorine radicals and long-lived radical precursors demonstrate that reactions involving bromine account for more than half of the catalytic destruction of ozone by halogens at ~20 km. In the air masses sampled, using the NASA ER-2 aircraft, bromine is 60 to 80 times more efficient on a per atom basis than chlorine at ozone removal. An inferred value for total stratospheric bromine agrees within error with measurements of the bromine source species, the organic bromine compounds that enter the stratosphere from the troposphere.

R. M. Stimpfle, D. W. Kohn, P. O. Wennberg, R. C. Cohen, T. F. Hanisco, J. G. Anderson, Department of Chemistry, Harvard University, Cambridge, MA 02138, USA.
R. J. Salawitch, Jet Propulsion Laboratory, Pasadena, CA 91109, USA
J. W. Elkins, Climate Monitoring and Diagnostics Laboratory, National Oceanic and Atmospheric Administration (NOAA), Boulder, CO 80303, USA.
D. W. Fahey, NOAA Aeronomy Laboratory, Boulder, CO 80303, USA.
R. S. Gao, M. H. Proffitt, NOAA Aeronomy Laboratory, Boulder, CO 80303 and CIRES, University of Colorado, Boulder, CO 80309, USA.
M. Loewenstein, K. R. Chan, National Aeronautics and Space Adminstration (NASA) Ames Research Center, Moffett Field, CA 94035, USA.

* To whom correspondence should be addresssed

Introduction

Bromine compounds contribute to halogen catalyzed ozone loss in the lower stratosphere with remarkable potency relative to more abundant chlorine compounds on a per atom basis (**1**, **2**). This increased efficiency arises from three causes. First, the organic source molecules (often referred to as CBr_y) that transport bromine from the troposphere to the stratosphere are relatively short-lived compared with chlorinated source gases (**3**). Thus in the stratosphere bromine is converted into forms capable of destroying ozone more rapidly than chlorine. Second, once bromine has been released from its source molecules, more than half is present during daylight in radical forms (BrO, Br) capable of efficient O_3 removal, whereas only a few percent of chlorine is present as radicals (**4**). Finally, the rates for two limiting reactions for catalytic O_3 loss involving bromine, $BrO + HO_2$ and $BrO + ClO$, are very rapid compared to rates for analogous reactions involving chlorine, $ClO + HO_2$ and $ClO + ClO$.

In 1987 the Montreal Protocol introduced provisions, further amended in London and Copenhagen, to regulate future emission of $CBrF_3$, $CBrClF_2$ and $C_2Br_2F_4$ (Halons 1301, 1211 and 2402), the industrially produced bromine compounds that posed the most substantial threat to the ozone layer. Approximately half of CBr_y is comprised of CH_3Br (methyl bromide) which has both natural and anthropogenic sources. Knowledge of the relative contribution of these two sources of CH_3Br is important to future regulatory decisions and is the subject of much controversy and uncertainty (**5**). Thus, while there is clear evidence from measurements of organic chlorine compounds in the troposphere that future O_3 loss by chlorine will likely decrease if the Protocol and its amendments are followed (**6**), the future course for bromine induced O_3 loss is unclear.

Measurements in the stratosphere are required to test hypotheses concerning the abundance and speciation of bromine compounds (7). Previous efforts have been hampered compared with similar work for chlorine compounds because atmospheric concentrations of bromine species are very low. Mixing

ratios of total CBr_y in the troposphere range from 16 to 30 pptv, whereas the corresponding concentration for chlorine compounds is ~ 3700 pptv (3). Here we present an analysis of in situ BrO measurements obtained in the lower stratosphere from the NASA ER-2 aircraft between February and November of 1994 during the Airborne Southern Hemisphere Ozone Experiment and Measurements for Assessing the Effects of Stratopheric Aircraft (ASHOE/MAESA) mission (8). Simultaneous measurements of hydrogen (OH and HO_2), nitrogen (NO and NO_2) and chlorine (ClO) radical species and long-lived tracers of atmospheric transport (CCl_3F, N_2O, CO_2, SF_6, $CBrClF_2$, O_3, H_2O and particles) are crucial for interpreting the BrO observations. Measurements of the rate limiting radicals in the dominant catalytic O_3 removal cycles allow the local O_3 destruction rate to be calculated (9).

In situ BrO measurements and tracer correlations

Measurements of [BrO] (10) are obtained by resonance fluorescence detection of Br atoms produced by the in situ titration of BrO with NO (11). The instrument is calibrated in our laboratory with known [Br], generated by reacting a known concentration of Cl atoms with excess Br_2. The estimated accuracy of the [BrO] measurements is ± 40% (2σ). The precision of an individual measurement is typically ± 2 pptv (2σ) using relatively long averaging times (~1 hour). The selection of averaging intervals is based upon simultaneous tracer measurements. Typically four to five measurements of [BrO] are produced for each eight hour flight.

Interpretation of the [BrO] measurements is aided by accurate estimates of the mixing ratio of inorganic bromine (Br_y). Similar to chlorine, we expect stratospheric [Br_y] to be non-linearly proportional to the integrated exposure of air parcels to ultraviolet radiation, which leads (either directly or indirectly) to production of Br_y from decomposition of source gases (12). Here we relate BrO (and Br_y) with the disappearance of organic source gases using CCl_3F (CFC-11), whose loss mechanism and loss rate are most similar to that of the aggregate of the organic bromine species (13).

All of the [BrO] measurements obtained during ASHOE/MAESA in daylight (solar zenith angles (SZA) < 85°) are plotted as a function of [CCl_3F] in the upper panel of **Fig. 1**. A relatively tight correlation between [BrO] and [CCl_3F] is observed even though a wide range of photochemical environments were encountered. The data were obtained during portions of winter, spring and fall in both the northern (to 59°N latitude) and southern (to 65°S latitude) hemispheres and for SZA ranging from 9° to 85°. We note that the maximum values of [BrO] measured here are approximately 50% larger than observed previously with this instrument **(14)**.

Halogen induced O_3 removal rates

The direct observation of [BrO], the rate limiting radical for catalytic destruction of O_3 by bromine compounds, obtained simultaneously with measurements of [HO_2], [ClO], [NO_2] and [O_3] provide a means to calculate the O_3 removal rate due to hydrogen, nitrogen, chlorine, bromine and oxygen containing species **(9)**. Here we focus on O_3 loss due to chlorine and bromine via the nine catalytic cycles listed in **Table 1**. The first reaction listed for each cycle is the rate limiting step for O_3 removal. For reactions having multiple pathways, only those leading to O_3 loss are listed. In parenthesis we give the approximate fraction of the total rate used here **(15)**.

The fractional contribution to the O_3 loss for each halogen cycle, computed from simultaneous observations of the radicals, is shown as a function of latitude in **Fig. 2 (16)**. The loss rates have been averaged over a 24 hr period using previously observed dependencies of radical concentrations with SZA **(9)**. This figure provides a snapshot of the 'observed' partitioning of O_3 loss between chlorine and bromine species for air masses sampled by the ER-2. It is of interest to note the predominance of the intra-halogen BrO+ClO cycle outside of the tropics. Bromine is involved in 55% to 65% of the total halogen induced loss rate **(17)**. The BrO+HO_2 rate limited cycle is the predominant bromine catalyzed O_3 loss cycle in the tropics.

Inorganic bromine partitioning

The ER-2 observations provide a means to evaluate the consistency of the BrO measurements with modeled partitioning of inorganic bromine (Br_y) and measurements of organic bromine (CBr_y). The daytime partitioning of Br_y is primarily controlled by the photochemical reactions shown in **Fig. 3**. The relative abundance of each reservoir is approximately proportional to the area of the box. It is noteworthy that each of the non-bromine reactants shown in **Fig. 3**, with the exception of formaldehyde (CH_2O), is measured simultaneously (**18**). The flux (pptv $hour^{-1}$) through each reaction path is given in parentheses for typical, mid-latitude conditions at ER-2 cruise altitudes (18 to 20 km). Photolysis rates are calculated from a radiative transfer model that takes into account variations in overhead ozone and albedo along the flight track of the ER-2 (**19**). Rate constants, absorption cross sections and quantum yields are taken from the JPL 1994 evaluation (**20**), except for recent work described below.

Recent laboratory work suggests important revisions in key photochemical processes that govern production and loss of $BrONO_2$ and HOBr. The heterogeneous reaction $BrONO_2 + H_2O \rightarrow HOBr + HNO_3$ on sulfate aerosol has beeen found to occur rapidly (**21**). This process does not strongly influence Br_y partitioning during the day, particularly when aerosol loading is light. The rate of the $BrO + HO_2$ reaction, the main production channel for HOBr, is approximately half the value recommended by the JPL 1994 evaluation (**22**). A consensus of new cross section measurements for HOBr photolysis, for which estimates had been based on aqueous phase spectra, leads to a value of $J_{HOBr} \sim 0.53 \times J_{HONO}$ (**23**). New cross section measurements of $BrONO_2$ photolysis lead to a 16% increase in its recommended J value (**24**). Taken together these changes increase the relative abundance of BrO within the Br_y family.

The very short lifetimes (< 15 min) of all the Br_y species except HBr permits the use of a model (as in **Fig. 3**) that assumes instantaneous photochemical stationary state (PSS) to predict the partitioning of Br_y (**25**). The inferred partitioning of BrO relative to the other Br_y gases is determined by

the first order photochemical reaction rates linking the Br_y species and is independent of measured [BrO] as well as knowledge of $[Br_y]$. The calculated partitioning is shown as a function of latitude in **Fig. 4**. The results have been filtered to illustrate the average trend with latitude. The PSS model predicts BrO is ~ 65% of $[Br_y]$ during daytime, nearly independent of latitude. $BrONO_2$ is predicted to be the second most abundant daytime species. HOBr is a small fraction of daytime $[Br_y]$, although at night heterogeneous hydrolysis of $BrONO_2$ on aerosols may convert nearly all Br_y to HOBr (**21**). In the tropics, the combination of low $[O_3]$ and $[NO_2]$ results in [Br] becoming a non-negligible fraction (10%) of $[Br_y]$, at the expense of $[BrONO_2]$. This analysis is consistent with the conclusions, drawn from measurements of [HBr] in the stratosphere (7), that HBr is a minor Br_y species in the lower stratosphere (**26**). Estimated values of [BrCl] and $[Br_2]$ are negligible at all latitudes during these observations.

A comparison of inorganic and organic bromine measurements

The measurements of [BrO] can be used to estimate $[Br_y]$ by scaling each [BrO] value by the predicted partitioning: $[Br_y]^{radical} = [BrO]^{measured} / ([BrO]/[Br_y])^{predicted}$, where $[Br_y]^{radical}$ denotes our estimate of $[Br_y]$ based upon observations of radicals. This estimate is important because it can be used to examine the consistency between observations of inorganic and organic bromine. Values of $[Br_y]^{radical}$ derived here are plotted as a function of $[CCl_3F]$ in the lower panel of **Fig. 1**. The solid line represents an estimate of $[Br_y]$ (denoted $[Br_y]^{source}$) based upon measurements of organic bromine compounds in the upper troposphere, $[CBr_y]^\circ$ ~ 18 ppt (**27**). The first order loss of CBr_y in the stratosphere is calculated relative to CCl_3F by adopting a loss rate for each organic bromine species based upon calculated photolysis rates and loss by reaction with OH (**28**). The dashed line is the estimated $[Br_y]^{source}$ that provides the best fit to the $[Br_y]^{radical}$ observations, given by assuming $[CBr_y]^\circ$ = 23 ppt. Although there is agreement between the $[Br_y]^{radical}$ observations and the best estimate of $[Br_y]^{source}$ (the solid line in **Fig. 1**), given the estimated error in $[Br_y]^{radical}$ (+80%, –45%), these [BrO] measurements and this analysis suggest there is ~ 30% more bromine in the stratosphere than indicated by the tropospheric

[CBr_y] measurements (29). The results summarized in Fig. 1. extend our quantitative understanding of the conversion of organic bromine to inorganic forms in the atmosphere and of the abundance of bromine in the atmosphere.

O_3 Loss by Halogens

To quantify the O_3 loss tendency of bromine relative to chlorine, the parameter 'α', given by the ratio of the sums of the individual loss rates involving bromine and chlorine, normalized by the respective abundances of the inorganic reservoirs, has been defined:

$$\alpha(\text{season, altitude, latitude}) = \frac{\sum_i k_i [BrO][X_i]}{[Br_y]} \Big/ \frac{\sum_j k_j [ClO][X_j]}{[Cl_y]} \qquad (1)$$

For bromine (chlorine) the index i (j) is summed over reactions 1-5 (5-9) of BrO (ClO) with reactant X_i (X_j) given in **Table 1**. α is a function of season, altitude and latitude, as well as other variables that can influence the partitioning of active and inactive forms of bromine and chlorine. These results provide a local, *instantaneous* measurement of α in the lower stratosphere ranging from values of 60 to 80, as shown in the lower panel of **Fig. 2**. [Br_y] is calculated from a fit of the $[Br_y]^{radical}$ observations derived here. [Cl_y] is calculated as a function of [CCl_3F] (30). **Fig. 2** provides direct confirmation of the effectiveness of Br_y relative to Cl_y in O_3 destruction in the lower stratosphere (31). Policy decisions regarding regulation of global emissions of CBr_y species require globally averaged values of α, a quantity that can only be provided by a model that integrates over latitude, season and altitude (32).

These observations demonstrate that bromine species are as important as chlorine species at contributing to halogen induced ozone removal in the lower stratosphere. The consistency among measurements of inorganic and organic bromine compounds gives confidence that our understanding of the partitioning and burden of bromine in the stratosphere is correct. However, more precise and accurate in situ measurements of all inorganic bromine species are required for more discriminating tests of bromine photochemistry. Significant questions remain concerning the importance of heterogeneous

reactions, especially in high aerosol loading environments following volcanic activity. Additional measurements of organic bromine compounds in the stratosphere and upper troposphere will increase our understanding of the process by which bromine is transported to and released in the stratosphere. The related issue of quantifying sources and sinks of organic bromine species (e.g., CH_3Br) in the troposphere is of paramount importance in obtaining a complete understanding of the role of bromine in the environment, and how that role depends on anthropogenic activity.

References and notes

1. S. C. Wofsy, M. B. McElroy and Y. L. Yung, *Geophys. Res. Lett.* 2, 215 (1975).
2. For a recent assessment of bromine in the atmosphere and other issues effecting the stratospheric ozone layer see: D. L. Albritton, R. T. Watson and P. J. Aucamp, *Scentific Assessment of Ozone Depletion: 1994, World Meteorological Organization Global Ozone Research and Monitoring Project, Report No. 37* (WMO, Geneva, 1995).
3. J. A. Kaye and S. A. Penkett, *Report on Concentrations, Lifetimes, and Trends of CFCs, Halons, and Related Species*, NASA Reference Publication 1339, January 1994.
4. The inorganic bromine species that efficiently participate in ozone destruction are often referred to as $Br_x = Br + BrO$. Total inorganic bromine is referred to as $Br_y = Br_x + BrONO_2 + HOBr + HBr + BrCl + 2Br_2$. Inorganic chlorine species are defined analogously: $Cl_x = Cl + ClO + 2ClOOCl$; $Cl_y = Cl_x + ClONO_2 + HOCl + HCl + 2Cl_2 + BrCl$. The ratio of Cl_x to Cl_y is typically only a few percent throughout most of the lower stratosphere during the day. It is only during the extraordinary situation observed in polar regions in late winter when Cl_x/Cl_y approaches 100%.
5. In addition to Ref. 2, see J. H. Butler, *Geophys. Res. Lett.* **21**, 185 (1994), S. A. Yvon and J. H. Butler, *ibid*, **23**, 53 (1996), M. A. K. Khalil *et al.*, *J. Geophys. Res.* **98**, 2887 (1993), J. M. Lobert *et al.*, *Science* **267**, 1002 (1995).
6. J. W. Elkins *et al.*, *Nature* **364**, 780 (1993) and R. G. Prinn *et al.*, *Science* **269**, 187 (1995).
7. For in situ observations of BrO see: W. H. Brune and J. G. Anderson, *Geophys. Res. Lett* **13**, 1391 (1986), W. H. Brune et al., *Science* **242**, 558 (1988), W. H. Brune et al., *J. Geophys. Res.* **94**, 16639 (1989), D. W. Toohey et al., *Geophys. Res. Lett.* **17**, 513 (1990), L. M. Avallone *et al.*, *ibid*, **22**, 831 (1995); For balloon-borne observations of HBr or HOBr: D. G. Johnson *et al.*, *Geophys. Res. Lett*, **22**, 1373 (1995), M. Carlotti *et al.*, *ibid*, **22**, 3207 (1995); For ground based column density observation of BrO: S. Solomon *et al.*, *J. Geophys. Res.* **94**, 11393 (1989), M. A. Carroll *et al.*, *ibid.*, **94**, 16633 (1989), K. H. Arpag *et al*, *ibid.*, **99**, 8175 (1994), A. Wahner and C. Schiller, *ibid.*, **97**, 8047 (1992), D. J. Fish *et al.*, *ibid.*, **100**, 18863 (1995).
8. ASHOE/MAESA flights took place from Moffett Field, California (37°N, 122°W); Barbers Point, Hawaii (22°N, 158°W); Nadi, Fiji (18°S, 178°E); and Christchurch, New Zealand (43°S, 173°E).
9. P. O. Wennberg *et al.*, *Science* **266**, 398 (1994).
10. Square brackets denote species concentration in density (molecules cm^{-3}) or mixing ratio (e.g., pptv, parts per trillion by volume) units.
11. W. H. Brune, J. G. Anderson, K. R. Chan, *J. Geophys. Res.* **94**, 16649 (1989), W. H. Brune, J. G. Anderson, K. R. Chan, *ibid*, **94**, 16639 (1989).
12. E. L. Woodbridge *et al.*, *J. Geophys. Res.* **100**, 3057 (1995), S. R. Kawa *et al.*, *ibid.*, **97**, 7905 (1992).
13. $[CCl_3F]$ is measured with the Airborne Chromatograph for Atmospheric Trace Species (ACATS-IV) instrument, accuracy = ±3%, J. W. Elkins *et al.*, *Geophys. Res. Lett.*, in press (1996). For flights where $[CCl_3F]$ measurements are not available observed $[CCl_3F]$ vs. $[N_2O]$ correlations from flights of similar latitude coverage are used to predict $[CCl_3F]$ from $[N_2O]$. $[N_2O]$ is measured by the Airborne Tuneable Laser Absorption Spectrometer (ATLAS), J. R. Podolske and M. Loewenstein, *Appl. Opt.*, **32**, 5324 (1993).

14. [BrO] measurements reported from the Airborne Artic Stratospheric Expedition II indicate [BrO] ~ 8 pptv whereas here we report [BrO] ~ 12 pptv for air of similar age, L. M. Avallone *et al.*, *Geophys. Res. Lett.* **22**, 831 (1995) and private communication. The origin of this difference, likely instrumental, is unidentified. Eliminating possible systematic differences in the [Br] calibrations as a source is problematic since, unlike [Cl] calibrations that are normalized to observed Rayleigh scattered signal, [Br] calibrations are specific to variables that can change with each mission, such as the magnitude of the chamber scatter signal. Also, inherently low signal-to-noise makes it difficult to identify systematic errors in flight data analysis. The magnitude of the discrepancy is not significantly greater than the overall [BrO] uncertainty which we estimate to be ± 40% ($\pm 2\sigma$)

15. For example, the BrO + ClO reaction has three known product channels: (1) BrCl + O_2, (2) Br + ClOO and (3) Br + OClO. The first two reactive paths make up catalytic cycles that destroy O_3 as shown in Table 1. The third path produces OClO, that is rapidly photolyzed to produce O + ClO. The O atom combines with O_2 to reform O_3 for every Br atom that reacts with O_3 to reform BrO, resulting in no net loss of O_3 for the third path.

16. O atom concentrations are calculated from the steady state expression:
$[O]^{ss} = J_{O3}[O_3]/(k_{O+O2}[O_2]+k_{O+O3}[O_3])$.

17. The presence of the BrO+ClO reaction complicates apportionment of the halogen induced O_3 loss rate between bromine and chlorine. The results of Fig. 2 show that ~ 55 to 65% of the calculated halogen loss is due to bromine while simultaneously ~ 60 to 50% is due to chlorine. From this perspective the partial derivative of halogen loss with respect to bromine at constant chlorine (or chlorine at constant bromine) is preserved.

18. [OH] and [HO_2] are detected by laser induced fluorescence, precision = ±0.05 pptv and ±0.2 pptv, accuracy = ±30% and ±40%, respectively, P. O. Wennberg *et al.*, *Rev. Sci. Instrum.* **65**, 1858 (1994); [NO] is detected by O_3 chemiluminescence, precision = ±0.02 ppbv, accuracy = ±15%, D. W. Fahey *et al.*, *J. Geophys. Res.* **94**, 11299 (1989) ; [NO_2] is detected by UV photolysis followed by O_3 chemiluminescence, precision = ±0.05 ppbv, accuracy = ±15%, R. S. Gao *et al.*, *ibid.* **99**, 20673 (1994); [ClO] is detected by UV resonance fluorescence, precision = ±4 pptv in 2 min, accuracy = ±35%, W. Brune et al., *ibid.*, **94**, 16649 (1989); [O_3] is detected by UV absorption, precision = ±0.06 ppbv at STP, accuracy = ±3%, M. H. Proffitt et al., *ibid.* **94**, 16547 (1989). All estimates are 2σ. The data are available on CD-ROM, S. E. Gaines, Ed., NASA Ames research Center, June 1995.

19. R. J. Salawitch *et al.*, *Geophys. Res. Lett.* **21**, 2551 (1994).

20. W. B. DeMore *et al.*, *Jet Propul. Lab. Publ.* **94-26** (1994)

21. D. R. Hanson and A. R. Ravishankara, *Geophys. Res. Lett.*, **22**, 385 (1995). The heterogeneous reaction of $BrONO_2 + H_2O \rightarrow HOBr + HNO_3$ is of great importance in controlling the relative abundances of $BrONO_2$ and HOBr during night. In addition this reaction alters the partitioning of nitrogen species and provides a source of hydrogen radicals.

22. The temperature dependence of the rate constant for the HO_2 + BrO reaction has recently been measured by three different groups: M. Larichev *et al.*, *J. Phys. Chem.* 99, 15911 (1995), M. Elrod *et al.*, submitted *J. Phys. Chem.* (1995) and Z. Li and S. P. Sander, private communication, 1995. The Elrod and Li results are approximately half the value of the Larichev results that formed the basis of the JPL '94 recommendation. For this analysis a value weighted towards the results of Elrod *et al.* and Li and Sander results is adopted, $k = 3.1\times10^{12}\exp(520/T)$.

23. Recent HOBr cross section measurements include: J. J. Orlando and J. B. Burkholder, *J. Phys. Chem.* 99, 1143 (1995); O. Rattigan, private communication, 1995, A. Sinha, private communication, 1995. We use the value from Orlando from 250 to 400 nm, extended by the

measurements of Sinha from 400 to 500 nm. The Rattigan value results in J values ~ 60% larger than the above composite result.

24. J. B. Burkholder *et al.*, *J. Geophys. Res.* **100**, 16793 (1995).

25. The PSS model calculation uses a steady state expression for $[NO_2]$ since direct measurements are not available for all flights :

$$[NO_2]^{ss} = 0.92 \times [NO]\left(k_{NO+O_3}[O_3]+k_{NO+ClO}[ClO]+k_{NO+BrO}[BrO]\right)/J_{NO_2}$$

The factor of 0.92 ±0.14 brings the value of $[NO_2]^{ss}$ into agreement with measured $[NO_2]$ for the flights for which we have [BrO] and $[NO_2]$ measurements. Although the magnitude of the disagreement is within the experimental error, we use the factor of 0.92 in order to base these calculations on the $[NO_2]$ measurement. See also: L. Jaegle *et al.*, *Geophys. Res. Lett.*, **21**, 2555 (1994) and R. S. Gao *et al.*, *J. Geophys. Res.* , submitted (1995).

The HBr calculation is an approximation since production (P) and loss (L) are too slow for steady state conditions to strictly apply. However if the ratio of P and L were integrated over the day the results would be nearly identical since P and L are functions of [OH] and $[HO_2]$ which have very similar diurnal behaviors. $[CH_2O]$ is estimated by assuming P = [CH4] × (k_{CH4+OH} [OH] + k_{CH4+Cl} [Cl]) and L = $[CH_2O]$ × J_{CH2O}. [Cl] is calculated from steady state: [Cl] = k_{ClO+NO} [ClO][NO]/k_{Cl+O3} $[O_3]$.

26. The balloon-borne HBr measurements (Ref. 7) indicate the yield of HBr from the $BrO+HO_2$ reaction cannot be more than a few per cent. An upper limit on the HBr yield measured in a laboratory is considerably less (0.01%), A. Mellouki et al., *J. Geophys. Res.*, 99, 22949 (1994).

27. The average value of the tropospheric input of organic bromine to the stratosphere in 1994 is taken as $[CBr_y]^\circ$ ~ 18 pptv. The average densities (pptv) of five CBr_y species measured in the upper troposphere near the tropics from the ER-2 aircraft in early 1992 (S. M. Schauffler *et al.*, *Geophys. Res. Lett.* **20**, 2567 (1993)) provide a measurement of $[CBr_y]$ = 17.7 pptv: $[CH_3Br]$ = 9.61, $[CBrF_3]$ = 2.77, $[CBrClF_2]$ = 2.88, $[C_2Br_2F_4]$ = 0.22 and $[CH_2Br_2]$ = 0.72. The values for $[CH_3Br]$ and $[C_2Br_2F_4]$ have been adjusted downward by 16% and 84%, respectively, due to calibration corrections (S. Schauffler, personal communication).

We have assumed growth of 0.14 and 0.15 pptv yr^{-1} for $CBrF_3$ and $CBrClF_2$, respectively, (J. Butler and S. Montzka, private communication) to adjust the Schauffler *et al.* measurements to 1994. Measurements from the NOAA Climate Monitoring and Diagnostics Laboratory (P. R. Wamsley, private communication) lead to a value of $[CBr_y]^\circ$ = 18.5 pptv.

28. The adopted first order loss rates (sec^{-1}) relative to a value of 1 for CCl_3F are: 3 (CH_3Br), 0.35 ($CBrF_3$), 3 ($CBrClF_2$), 3.4 ($C_2Br_2F_4$) and 10 (CH_2Br_2). The relative loss rates are based on 24 hour averaged values of calculated photolysis rates (Ref. 18) and [OH] in the lower stratosphere. An age of air correction has been applied assuming a $[CBr_y]^\circ$ growth rate of 1.7 % yr^{-1} (NOAA CMDL) and a maximum age of air of four years.

29. More accurate estimates of $[Br_y]$ are available from analyses based on measurements of CBr_y compounds in the stratosphere. Measurements of $[CBrClF_2]$, $[CCl_3F]$ and $[SF_6]$ by ACATS-IV (ref. 13) during ASHOE/MAESA have been used to determine the total bromine budget in the stratosphere (P. R. Wamsley *et al.*, *J. Geophys. Res.*, in prep., 1996). The peak $[Br_y]$ values calculated using the ACATS-IV data are ~ 12% less than the $[Br_y]^{source}$ calculation (the solid line in Fig. 1) presented here (P. R. Wamsley, private communication). Estimates of $[Br_y]$ for other time periods are available from whole air sampling from the ER-2 aircraft (S. Schauffler, private communication).

30. For $[Cl_y]$ in ppbv and $[CCl_3F]$ in pptv, for latitudes poleward of 10° N or S, $[Cl_y] = 2.764 - 1.057\times10^{-2}$ $[CCl_3F] + 4.055\times10^{-6}$ $[CCl_3F]^2$ for $18<[CCl_3F]<276$; equatorward of 10° N or S, $[Cl_y] = 2.478 - 8.640\times10^{-3}$ $[CCl_3F]$ for $230 \le [CCl_3F] \le 276$, and $[Cl_y] = 2.752 - 9.83\times10^{-3}$

$[CCl_3F]$ for $18 \leq [CCl_3F] \leq 230$. The ACATS instrument measures five organic chlorine species that make up 80% of total organic chlorine.

31. It is important to note that the absolute reaction rates used to calculate the results of Fig. 2 are much lower in the tropics than at mid and high latitudes. The tropics are net O_3 producing regions, while the mid and high latitudes are net O_3 loss regions.

32. Since α is steeply dependent on altitude (z), peaking at very low values of z, a globally integrated value will likely be smaller than a local measurement in the lower stratosphere. A typical model calculation at mid-latitudes predicts $\alpha(z = 20 \text{ km}) \sim 100$, R. R. Garcia and S. Solomon, *J. Geophys. Res.*, **99**, 12937 (1994). However, comparison of these results with model calculations must be made cautiously if model input parameters are not matched to those characteristic of these measurements and this analysis.

33. The authors wish to acknowledge the pilots and ground crew of the NASA ER-2 without whose dedication these measurements would not be possible. We thank A. Sinha, M. Elrod and Z. Li for sharing prepublished results concerning HOBr cross section or HO_2+BrO rate constant measurements and S. Schauffler for updated organic bromine measurements. Project scientists for ASHOE/MAESA were A. Tuck for ASHOE and W. Brune for MAESA. Sponsorship of ASHOE/MAESA came from NASA's Upper Atmospheric Research Program, M. Kurylo program manager, and Atmospheric Effects of Aviation Project, H. Wesoky program manager.

Figure Captions.

Fig.1. Upper panel, [BrO] vs. [CCl_3F] for all ASHOE/MAESA flights where SZA < 85°. Lower panel, $[Br_y]^{radical}$ vs. [CCl_3F] where $[Br_y]^{radical}$ denotes our estimate of [Br_y] based upon observations of radicals. The solid line represents $[Br_y]^{source}$ based upon measurements of organic bromine compounds in the upper troposphere, $[CBr_y]^\circ$ = 18 ppt. The dashed line provides the best fit of $[Br_y]^{source}$ to observed $[Br_y]^{radical}$ calculated by assuming $[CBr_y]^\circ$ = 23 pptv. The open circle denotes the tropospheric value of [CCl_3F] = 272 pttv.

Fig. 2. Upper panel, the observed fractional contribution of the halogen catalyzed ozone loss cycles listed in Table 1 (identified by the rate limiting step) vs. latitude. The contributions from the BrO + O, BrO + BrO and BrO + NO_2 reactions have been combined for clarity. Contribution from the ClO + ClO reaction is insignificant for these data. Lower panel, α vs. latitude.

Fig. 3. The primary bromine photochemical reactions in daylight. For bromine compounds, box areas are approximately proportional to abundances. Non-bromine reactants are identified near the arrows. Fluxes (pptv hr^{-1}) for each path are given in parentheses for the typical conditions: T=215 K, [M] = 2×10^{18} molec cm^{-3}, [HO_2] = 4 pptv, [OH] = 0.75 pptv, [O_3] = 2 ppmv, [NO] = 200 pptv, [NO_2] = 200 pttv, [ClO] = 30 pptv, [CH_4] = 1.5 ppmv and [Br_y] = 17 pptv.

Fig. 4. The partitioning of inorganic bromine (Br_y) calculated using the PSS model vs. latitude. [BrCl] and [Br_2] are insignificant for these data.

Table 1. Halogen catalyzed ozone loss cycles.

1. $\mathbf{BrO + HO_2 \longrightarrow HOBr + O_2}$
$HOBr \xrightarrow{h\nu} OH + Br$
$OH + O_3 \longrightarrow HO_2 + O_2$
$Br + O_3 \longrightarrow BrO + O_2$

2. $\mathbf{BrO + BrO \longrightarrow 2Br + O_2}$ (.6)*
$\longrightarrow \mathbf{Br_2 + O_2}$ (.4)
$Br_2 \xrightarrow{h\nu} 2Br$
$2Br + 2O_3 \longrightarrow 2BrO + 2O_2$

3. $\mathbf{BrO + NO_2 \xrightarrow{M} BrONO_2}$
$BrONO_2 \xrightarrow{h\nu} Br + NO_3$ (.5)
$NO_3 \xrightarrow{h\nu} NO + O_2$ (.1)
$Br + O_3 \longrightarrow BrO + O_2$
$NO+O_3 \longrightarrow NO_2 + O_2$

4. $\mathbf{BrO + O \longrightarrow Br + O_2}$
$Br + O_3 \longrightarrow BrO + O_2$

5. $\mathbf{BrO + ClO \longrightarrow BrCl + O_2}$ (.05)
$\longrightarrow \mathbf{Br + ClOO}$ (.4)
$BrCl \xrightarrow{h\nu} Br + Cl$
$ClOO \xrightarrow{M} Cl + O_2$
$Br + O_3 \longrightarrow BrO + O_2$
$Cl + O_3 \longrightarrow ClO + O_2$

6. $\mathbf{ClO + HO_2 \longrightarrow HOCl + O_2}$
$HOCl \xrightarrow{h\nu} OH + Cl$
$OH + O_3 \longrightarrow HO_2 + O_2$
$Cl + O_3 \longrightarrow ClO + O_2$

7. $\mathbf{ClO + ClO \xrightarrow{M} ClOOCl}$
$ClOOCl \xrightarrow{h\nu} Cl + ClOO$
$ClOO \xrightarrow{M} Cl + O_2$
$2Cl + 2O_3 \longrightarrow 2ClO + 2O_2$

8. $\mathbf{ClO + NO_2 \xrightarrow{M} ClONO_2}$
$ClONO_2 \xrightarrow{h\nu} Cl + NO_3$ (.9)
$NO_3 \xrightarrow{h\nu} NO + O_2$ (.1)
$Cl + O_3 \longrightarrow ClO + O_2$
$NO+O_3 \longrightarrow NO_2 + O_2$

9. $\mathbf{ClO + O \longrightarrow Cl + O_2}$
$Cl + O_3 \longrightarrow ClO + O_2$

* The approximate yield for a given reaction is listed in parenthesis where applicable.

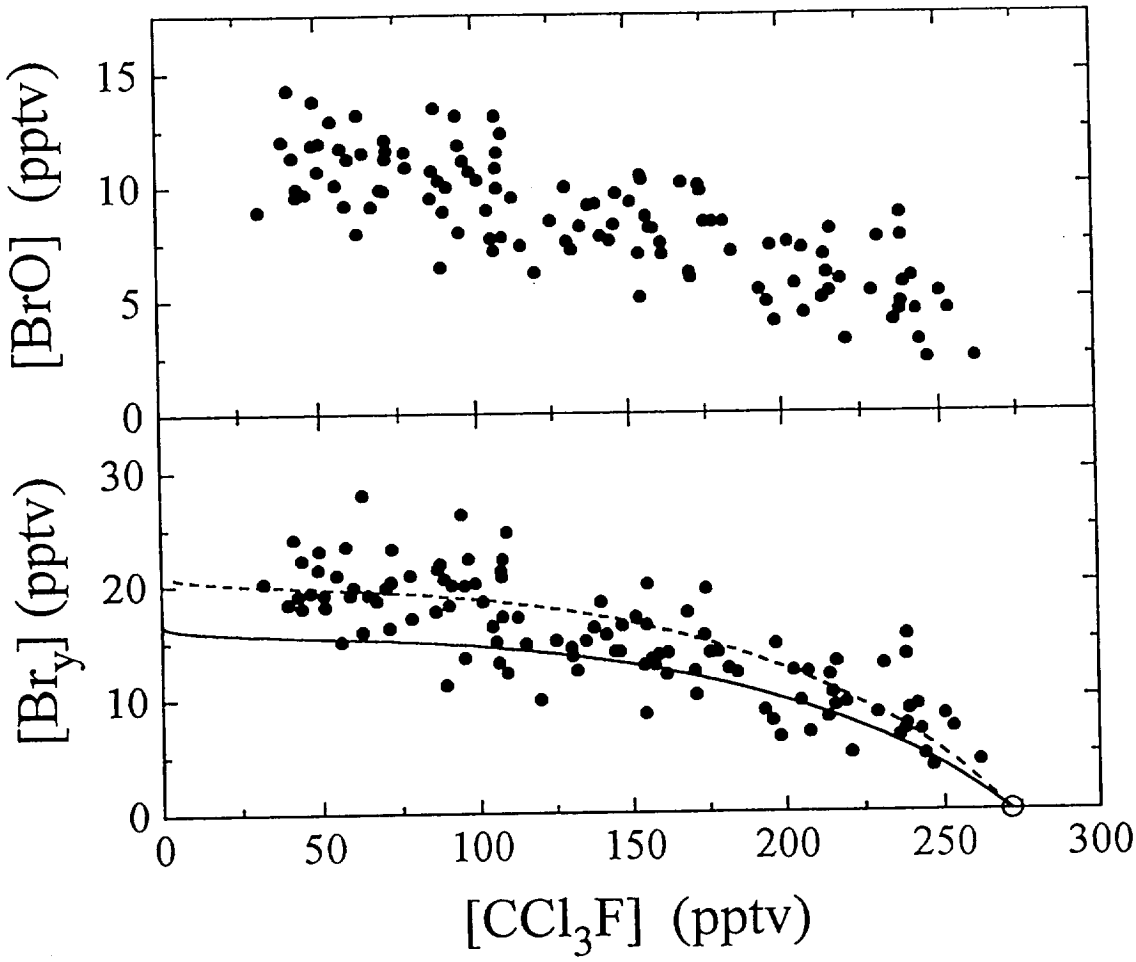
[BrO] (pptv)
15
10
5
0
[Br$_y$] (pptv)
30
20
10
0
0
50
100
150
200
250
300
[CCl$_3$F] (pptv)

Fig. 1.

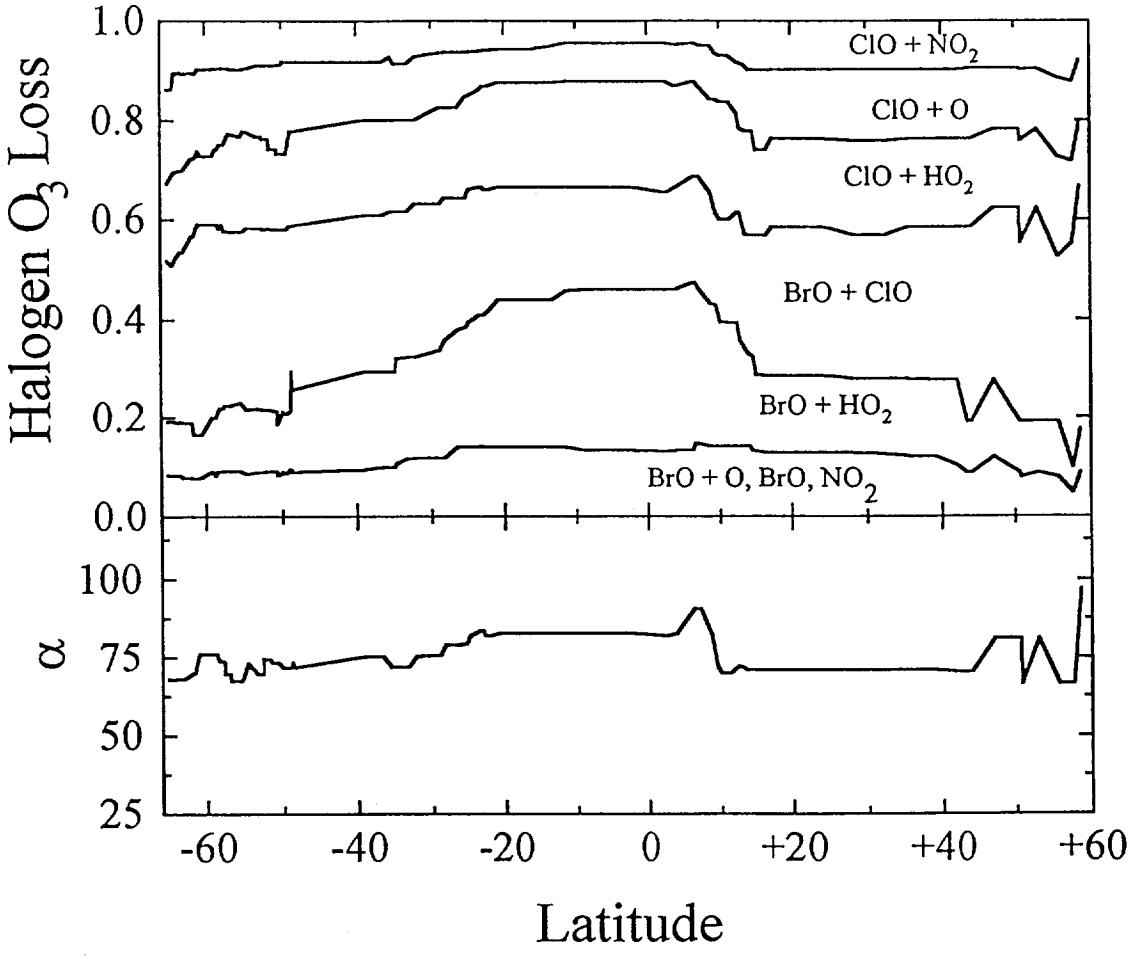
Halogen O_3 Loss
1.0
0.8
0.6
0.4
0.2
0.0
ClO + NO_2
ClO + O
ClO + HO_2
BrO + ClO
BrO + HO_2
BrO + O, BrO, NO_2
α
100
75
50
25
-60
-40
-20
0
+20
+40
+60
Latitude

Fig. 2.

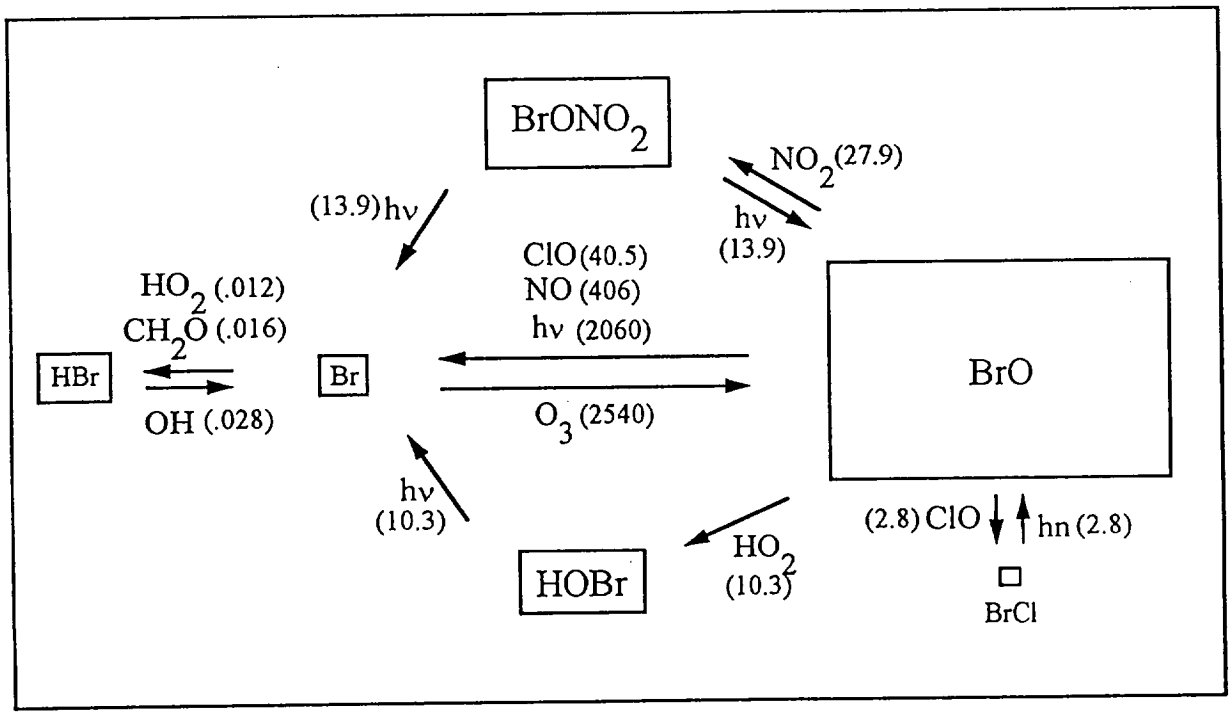
BrONO2
NO2 (27.9)
(13.9) hν
hν
(13.9)
ClO (40.5)
NO (406)
HO2 (.012)
CH2O (.016)
hν (2060)
HBr
Br
BrO
OH (.028)
O3 (2540)
hν
(10.3)
(2.8) ClO
hn (2.8)
HO2
(10.3)
HOBr
BrCl

Fig. 3.

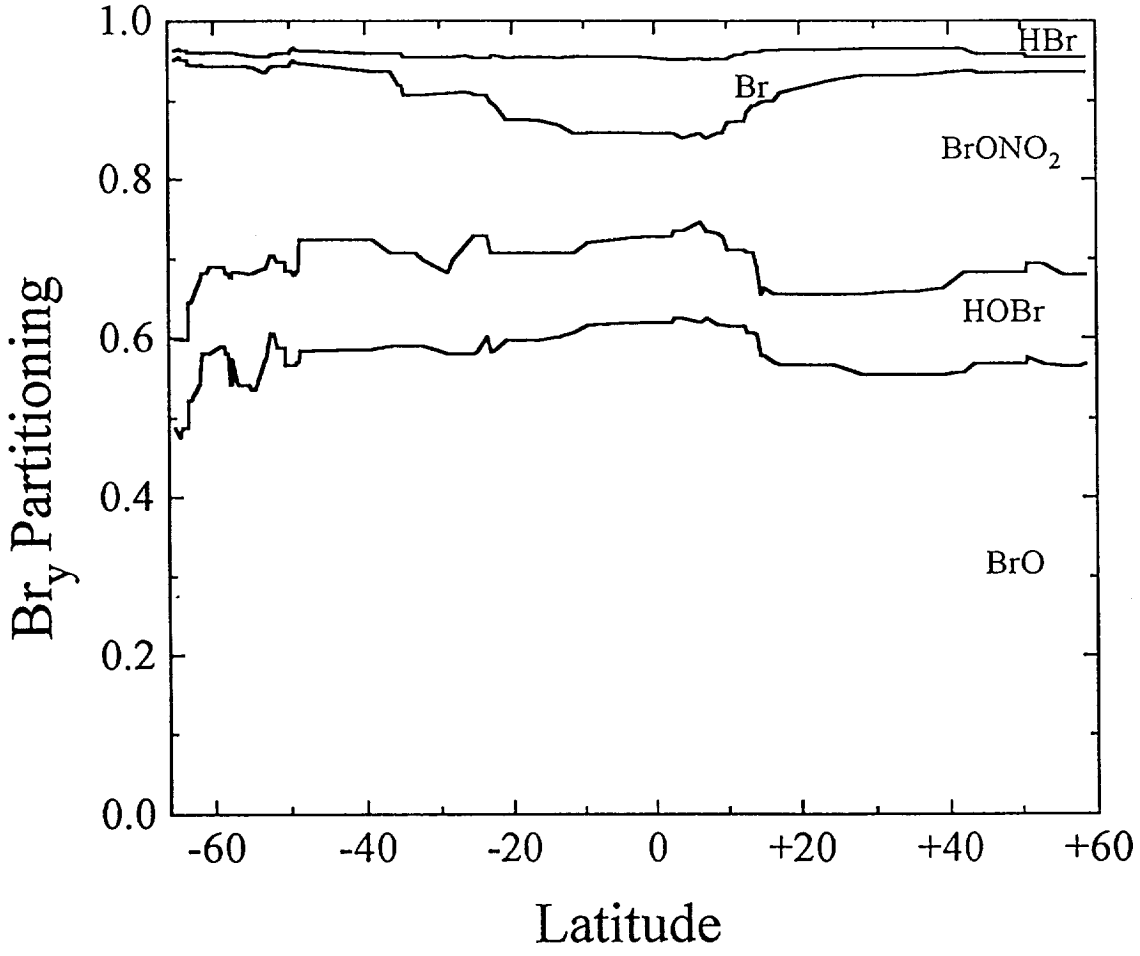
1.0
0.8
0.6
0.4
0.2
0.0
Br_y Partitioning
-60
-40
-20
0
+20
+40
+60
Latitude
HBr
Br
$BrONO_2$
HOBr
BrO

Fig. 4.

In preparation for submittal to Science, 1996

In Situ Measurements of HOx in Super- and Subsonic Aircraft Exhaust Plumes.

by

T. F. Hanisco[1], P. O. Wennberg[1], R. C. Cohen[1], J. G. Anderson[1], D. W. Fahey[2], E. R. Keim[2,3], R. S. Gao[2,4], R. C. Wamsley[2,4], S. G. Donnelly[2,4], L. A. Del Negro[2,4], R. J. Salawitch[5], K. K. Kelly[2], and M. H. Proffitt[2].

[1]Department of Chemistry, Harvard University, Cambridge, MA 02138.
[2]Aeronomy Laboratory, National Oceanic and Atmospheric Administration, Boulder, CO 80303.
[3]NASA Ames Research Center, Moffett Field, CA 94035.
[4]Cooperative Institute for Research in Environmental Science, University of Colorodo, Boulder, CO 80309.
[5]Jet Propulsion Laboratory, California Institute of Technology, Pasadena, CA 91109.

Abstract

Concentrations of OH and HO_2 have been measured in the exhaust of an Air France Concorde and a NASA ER-2 in the lower stratosphere. Analysis of these results shows that OH and HO_2 concentrations downstream of the exhaust point are determined by the emission index of NOx (NO + NO_2), OH and HONO. Reactive hydrogen emissions (the sum of OH and HONO) are 5% of the NOx emission from both aircraft, indicating that the factors that control OH and NOx emissions from each engine are similar. The measurements of OH imply that only a small fraction of NOx (5%) and SO_2 (1%) are oxidized in the the plume of the Concorde. These measurements constrain the production rates of nitric and sulfuric acid particles in the plume that may partially determine the perturbation to stratospheric ozone by a fleet of super-sonic aircraft.

Introduction

The emissions from a proposed fleet of commercial high speed civil transports (HSCT's) may alter the distribution of stratospheric ozone. In 1971 concerns that reactive nitrogen (NOx) emissions would substantially deplete ozone helped deter the development of HSCT's in the U. S. Recent observations of the exhaust from an Air France Concorde during supersonic flight in the lower stratosphere showed that the measured NOx concentrations agreed well with predictions based on ground-based tests performed in the early 70's. However, the number of volatile particles measured (assumed to be sulfate aerosols) is substantially higher than expected. Reactions on sulfate aerosols regulate the abundance of the hydrogen, halogen, and nitrogen radical families that catalyze ozone loss. Perturbations to the global aerosol distribution by a proposed fleet of HSCT's could lead to a level of ozone depletion comparable to that expected from NOx emissions alone. It has long been assumed that the initial step in sulfate aerosol formation is the oxidation of emitted SO2 in the aircraft exhaust wake. Estimates of oxidation rates range from significant to insignificant values, depending on the assumptions of the chemistry of OH. We present observations of OH in the wake of the Concorde. The measured concentrations of OH are insufficient to account for the particle numbers reported by Fahey, et. al.

Recent in situ measurements of the Concorde exhaust determined the emissions of some key exhaust species: CO_2, H_2O, NO, NO_2, CO (3). The agreement between the in situ measurements and extrapolations from ground based tests establishes a high level of

confidence in the methods that will be used to predict emissions of these species from new engine designs. However, the concentrations of highly reactive emissions, such as reactive hydrogen (HOx = H, OH, HO_2), are difficult to measure accurately in test chambers. Other species, such as nitric acid ($HONO_2$) and sulfuric acid (H_2SO_4), will form in the exhaust plume after emission, thus their concentrations are nearly impossible to measure in test chambers. The lack of experimental data has resulted in decades of speculation based on models of aircraft plume chemistry in which acid production rates range from insignificant (4) to significant (5,6) values depending on the assumptions of the chemistry of HOx in each model.

Knowledge of the production of these species from HSCT exhaust is required due to their important role in heterogeneous processes contributing to ozone loss. Sulfuric acid is the precursor to sulfate aerosols that participate in the partitioning of reactive nitrogen species (NOy = NOx + $HONO_2$ + N_2O_5 + HO_2NO_2 + $ClONO_2$...). Nitric acid can potentially form acidic particles that contribute to the partitioning of halogen species (7,8). Since particle formation rates are non-linear with respect to acid concentrations the net perturbation to heterogeneous chemistry from aircraft emissions in the lower stratosphere will depend on local plume chemistry where acid concentrations are high. For example, the calculated perturbation to sulfate aerosol surface area from a fleet of 500 HSCT's depends on whether sulfate aerosols form within the plume or whether emitted sulfur accomodates on preexisting particles (3). Similarly, the probability of nitric acid particle formation increases dramatically if high concentrations of nitric acid are formed in the plume prior to dispersal (6).

The evolution of OH in the plume will determine the production rate of nitric and sulfuric acid before the plume disperses. As shown in Fig. 1, reactive hydrogen is emitted as OH and nitrous acid (HONO), which is formed in the engine exhaust via (9):

$$OH + NO + M \rightarrow HONO \qquad (1)$$

Within seconds of emission, the emitted OH completely reacts with emitted NO to form HONO. During daylight, HONO is photolyzed to OH and NO with a time constant of 6 minutes (10). Hence, HONO acts as a temporary reservoir for the OH produced in the engine.

The production of nitric and sulfuric acid in the plume occurs as the plume ages through the reactions:

$$OH + NO_2 + M \rightarrow HONO_2 \qquad (2)$$

$$OH + SO_2 + M \rightarrow HOSO_2 \xrightarrow{O_2} SO_3 \xrightarrow{H_2O} H_2SO_4 \qquad (3)$$

In reaction 3, $HOSO_2$ is quickly converted to the more stable SO_3, which is converted to H_2SO_4 (11). Measurements of OH can be used to calculate the amount of nitric and sulfuric acid formed in the plume and to show that these formation rates decrease to background levels within an hour. In addition, simultaneous measurements of the chemical species that contribute to plume chemistry can confirm the chemical description in Fig. 1 and establish an empirical basis for the models predicting plume chemistry and dynamics.

HOx Measurements

The measurements presented here were obtained aboard the NASA ER-2 during the 1994 Airborne Southern Hemisphere Ozone Experiment/Measurements for Assessing the Effects of Stratospheric Aircraft (ASHOE/MAESA) campaign in Christchurch, New Zealand. The instrument payload included instruments measuring most of the species necessary to empirically test HOx chemistry: NO, NO_2, NOy, BrO, ClO, OH, HO_2, H_2O, O_3, CH_4, CO, pressure, temperature, and spectrally resolved radiation fields.

The HOx instrument is described in detail by Wennberg, *et al.* (12). Briefly, a controlled flow of air is ducted into the nose of the ER-2. The OH radical is measured in a wall-less sampling region by laser induced fluorescence (LIF) and HO_2 is measured after chemical conversion to OH by reaction with NO. The residence time of OH in the sampling region is less than 1 ms and the LIF signal is recorded at 8 Hz. At ER-2 cruising speed this sampling rate corresponds to 25 m spatial resolution. The precision and accuracy (1σ) of the OH and HO_2 measurements at 8 Hz are 0.1 ppt, ±30% and 0.2 ppt, ±40%, respectively. The HOx instrument was modified prior to the ASHOE/MAESA campaign to provide simultaneous measurements of OH and HO_2 with two identical LIF detection axes (13).

The encounter with the Concorde was arranged by ER-2 and Air France pilots and operations personnel. The encounter began at approximately 2:45 pm local time on October 8, 1994 above the east coast of New Zealand. A few minutes after the Concorde passed the prearranged rendezvous, the ER-2 traced a 320 km portion of the Concorde flight path three times in 90 minutes and crossed the exhaust plume at least 11 times. During the return into Christchurch the ER-2 crossed its own wake after a turn. Data for

OH and HO_2 were obtained for 5 of the Concorde plume crossings and the single ER-2 plume crossing. The age of the plume at each intercept is determined from position information provided by the Concorde pilots, a ground based radar tracking station, and the ER-2 instrumentation. The plume intercepts occurred at 16.2 km altitude (100 mbar) where the temperature was 222 K. Three of the intercepts correspond to emission during the Concorde cruise at Mach 2 and two correspond to emission at Mach 1.7.

Figure 2 shows the OH and HO_2 mixing ratios measured during three crossings of the Concorde exhaust plume (a-c) and the single encounter with the ER-2 plume (d). The encounters occurred at Greenwich times of 10384 s, 12697 s, 12964 s, and 15564 s. The plumes ages are 16, 60, and 66 minutes for the Concorde and 10 minutes for the ER-2. The OH measurement shows that the profile of the plume is quite uniform and has very sharp edges, especially the largest Concorde plume shown in Fig. 2a. The **duration** of this plume is 2.65 s, which corresponds to a 530 m cross section of the plume. If a 30° angle of incidence between the ER-2 and Concorde flight tracks is assumed, the plume is roughly 265 m wide.

As the plume ages, the concentration of OH falls markedly. In the young plumes (eg. Figs. 1a and 1d) the concentration of OH is above ambient because the production of OH from the photolysis of HONO is large. In the older plumes (eg. Fig. 1c) the concentration of OH decreases because the concentrations of HONO are diminished and the loss rate of OH due to reactions 1 and 2 is still large (14). The small concentration of HO_2 in the plume results from a change in the partitioning of HOx (15). HO_2 is converted to OH via the reaction

$$HO_2 + NO \rightarrow NO_2 + OH \qquad (4)$$

The high concentrations of NO in the plume shift the partitioning of HOx towards OH because the concentrations of species that convert OH to HO_2 (O_3 and CO) do not increase above background levels inside the plume. The concentrations of NO are much lower in the ER-2 plume (Fig. 1d), thus a much smaller change in the partitioning between OH and HO_2 is observed.

The Hydrogen Radical Emission Index

Because of the short lifetime of OH in the atmosphere, we expect the OH that is emitted from the engine to disappear within a few seconds after emission. The observed

increase in the concentrations of OH within the plume 1000 seconds after emission indicates that there is a significant amount of HONO in the plume at the time of measurement. We can infer the concentration of HONO in the plume by comparing production and loss rates calculated with a steady state photochemical model. We calculate the rates outside the plume as well in order to test the steady state model. Since the lifetime of OH is short, production and loss rates calculated with this model should be equal. For the calculation inside the plume, we determine the concentration of HONO required to balance production and loss rates.

The production and loss rates of OH during plume #3 (Fig. 1a) calculated using measurements obtained aboard the ER-2 (16), rate constants from DeMore *et al.* (17), and photolysis rates calculated with a radiative transfer model (18) are listed in Table 1. Outside the plume the agreement between production and loss rates is excellent. This agreement is consistent with the steady state condition and indicates that the chemistry used in the model sufficiently describes the production and loss rates of ambient OH. Inside the plume, loss rates increase by two orders of magnitude due to the large increases in NO and NO_2 concentrations, but the increase in production rates due to background species (H_2O, HO_2NO_2, H_2CO) is small. In order to balance the increase in loss rates a large amount of HONO must be added to the model. The concentration of HONO in the plume inferred from this comparison is 165 ± 65 ppt (1σ). Since the loss rates of OH in the plume are dominated by reactions 1 and 2, the uncertainty of this estimate of HONO is determined by uncertainties in the OH, NO, and NO_2 measurements, rate constants of reactions 1 and 2, and the photolysis rate of HONO. The contribution of other sources of OH formed in the exhaust are neglected in this estimate, but will be addressed in detail below.

The amount of HONO formed in the exit plane of the engine from emitted OH can be determined once the loss rate of HONO in the plume is known. Because of the high concentrations of NO and NO_2 in the plume the net loss rate of HONO is described by HONO, OH, and NOx chemistry. HONO is lost through photolysis and regenerated through reaction 1. The net sink for HONO is nitric acid:

$$HONO \underset{NO}{\overset{h\nu}{\rightleftarrows}} OH \xrightarrow{NO_2} HONO_2 \qquad (4)$$

The net loss rate for HONO in the plume is the fraction of photolyzed HONO that forms nitric acid multiplied by the photolysis rate:

$$loss_{HONO} = \frac{k_2[OH][NO_2]}{k_1[OH][NO] + k_2[OH][NO_2]} \times J_{HONO}[HONO] \quad (5)$$

The concentration of HONO formed in the exhaust via reaction 1 can be estimated by integrating the loss rate of HONO over the age of the plume and correcting for the effects of dilution. This amount of HONO corresponds to the sum of emitted OH that forms HONO via reaction 1 after emission and any HONO that might be directly emitted from the engine (19). We represent this sum (OH + HONO) as HOy. Dilution effects can be removed by referencing to a conserved tracer, such as NOy:

$$\frac{HOy}{NOy} = \frac{\int_0^t loss_{HONO} dt}{NOy} \quad (6)$$

For the conditions of plume #3 the amount of HOy at the time of exhaust is 0.045×NOy.

The uncertainty of the estimate of the amount of HOy emitted from the engine calculated from Eq. 6 depends on the fraction of emitted OH that forms HONO. The extremely fast reactions of OH with NO and NO_2 and the high levels of NOx in the plume ensure that nearly all of the emitted OH will react with NOx. The oxidation of SO_2 discussed below is catalytic with respect to OH (11) and would not account for OH loss even if sulfur emissions were as large as NOx emissions. The main uncertainty is whether the emitted OH reacts with NO or NO_2. Ground based test cell measurements of the Olympus engine indicate that NO_2 is only 4% of total emitted NOx at the engine exit plane (20). Based on the rates of reactions 1 and 2, this fraction of NO_2 contributes an additional uncertainty of ±10% to the ratio HOy/NOy calculated from Eq. 6, resulting in a net uncertainty of ±50% (1σ). If other loss processes for emitted OH occur, the amount of OH estimated from equation 6 will be a lower limit.

The time evolution of OH in the plume was calculated with an integrating photochemical model. The model exactly solves the coupled differential equations that control OH concentrations. The inputs to the model are measured concentrations and temperatures, calculated photolysis rates, and the concentration of HONO calculated from Eq. 6. The results using initial HOy/NOy = 0.045 and the conditions measured for plume #3 are shown in Figure 3a. The first data point corresponds to the OH concentration

measured for plume #3. The other data points correspond to OH concentrations measured during later encounters, scaled by the amount of NOy in the plume to account for dilution. The agreement of this model with the measured OH for plume #3 shows that the assumptions in the calculation of HONO discussed above are consistent, at least for the early plumes. Contributions to HOx chemistry from species other than HONO and NOx are only few percent at 15 minutes after emission. The curvature after 30 minutes occurs because other processes, mostly HO_2NO_2 photolysis, contribute to the production of OH. However, the rates of these processes are small compared to the loss rates due to reaction 2, and the concentration of OH drops significantly below background levels (see Fig. 2c).

The decrease in the concentration of OH after 30 minutes has important implications for the chemistry of OH within the plume. That is, the enhancement of oxidation rates due to OH in the plume is complete within 30 minutes or so. To illustrate this point, Figs. 3b and c show the fractions of emitted NOy and SOx that are oxidized by OH within the plume via reactions 2 and 3. Roughly 5% of NOx and 1% of SOx are oxidized by OH in the plume, mostly within the first 15 minutes. An additional 0.8% of SOx would be oxidized prior to HONO formation if all the HOy were emitted as OH. The small fraction of oxidized NOx is consistent with the near unity NOx/NOy ratio measured by Fahey, *et al.* (3).

After 60 minutes, most of the HONO is gone, and OH production rates return to background levels (~5 ppq/s). Since the oxidation rates of NO_2 and SO_2 are limited by the OH production rate, the maximum oxidation rate of NO_2 and SO_2 is only ~5 ppq/s for plume ages greater than 1 hour. At these rates NOx and SOx will have a lifetime with respect to OH oxidation determined by the photochemistry of the stratosphere and not the local chemistry within the plume. For aircraft emissions occurring during the night gas-phase oxidation of NO_2 and SO_2 may not occur, and the heterogeneous removal of HONO by sulfate aerosols may become important (10).

Discussion

Table II summarizes the measurements of the Concorde and ER-2 exhaust plumes. The Concorde encounters include exhaust emitted at Mach 2 (#3) and Mach 1.7 (#4 and #5). The ER-2 emission indices represent an average of 3 plume encounters during SPADE (21) and 4 encounters during ASHOE/MAESA. The HOy/NOy ratio calculated from Eq. 6 and the emission indices (EI) of NOy, expressed in grams of NO_2,

and HOy, in grams of OH per kilogram fuel are listed. Since essentially all of the HOy emitted from the engine is converted to $HONO_2$, the HOy/NOy ratio represents the fraction of emitted NOy converted to nitric acid in the plume. These ratios are consistent with the near unity NOx/NOy ratios reported for these encounters (3). Both the HOy EI and the NOy EI (3,22) are substantially smaller for the ER-2 and Mach 1.7 cases than for the Mach 2 case. This trend is consistent with the strong temperature dependence of OH and NO emission indices (23,24). The Concorde engine (Olympus 593, exhaust gas temperature (EGT) = 680°C) runs hotter than the ER-2 engine (Pratt & Whitney J75, EGT = 600°C) and produces substantially more NO in the exhaust (3,22).

Interestingly, the HOy/NOy ratios are nearly constant for both engines and both operating conditions of the Concorde. This result indicates that the factors that control OH and NO emission have similar temperature dependencies- a result that is not obvious, considering the complexity of the chemistry involved inside the engine. Whether HOy/NOy is constant in general is worth investigating because this ratio determines the fraction of NOx that is oxidized in the plume. Efforts are currently underway to develop HSCT engines with significantly lower NOy EI's than the Concorde Olympus 593 (25). If HOy emissions do not scale similarly to NOy emissions, there will be different oxidation ratios in the plume. Since HOy determines the amount of nitric acid in the plume, the probability of nitric acid particle formation will depend on HOy emission levels (6). Thus, the probability that nitric acid particles form before the plume disperses will not decrease unless HOy emissions are lowered as well.

Measurements of particle numbers in the Concorde plume, thought to be composed of primarily sulfuric acid aerosols, imply that at least 10-40% of sulfur in the fuel is oxidized to H_2SO_4 (3). However, HOx measurements suggest that only 1-2% of SO_2 is oxidized by OH via gas-phase reactions in the plume. Thus, a clear discrepancy exists between the amount of H_2SO_4 inferred from particle measurements and the amount of sulfur that can be oxidized by OH in the plume. The discrepancy could be resolved if the particles are not composed primarily of H_2SO_4 or if the sulfur is oxidized in the engine prior to emission. It is important to determine whether large amounts of sulfur are oxidized in the engine and if this oxidation will occur for low NOx engines as well. Whether sulfur is emitted as SO_3, which quickly forms H_2SO_4 (11), or as SO_2 will determine whether sulfate aerosols form in the plume or long after the plume disperses. This formation rate directly affects the size distribution of sulfate aerosols, and will determine the impact of sulfate emissions on global aerosol surface areas (3).

Table 1. Production and loss rates of OH for the conditions of plume #3. Rates are in parts per quadrillion (1 ppq = 10^{-15} mol/cm^3) per second.

	Background rate (ppq/s)	% of total	Plume rate (ppq/s)	% of total
OH Production				
$HONO_2 + h\nu$	1.06	26	1.4	0
$H_2CO + h\nu$	1.06	26	3.0	1
$O(^1D) + H_2O$	0.88	22	1.0	0
$HONO + h\nu$	0.39	10	447	98
$HO_2NO_2 + h\nu$	0.33	8	2.9	1
total	4.24		455	
OH Loss				
$OH + HO_2$	0.97	21	1.6	0
$OH + NO_2$	0.88	19	258	57
$OH + HONO_2$	0.85	19	4.2	1
$HO_2 + NO_2$	0.67	14	11.8	3
$OH + NO$	0.39	9	155	34
$OH + HO_2NO_2$	0.36	8	9.7	2
total	4.54		455	

$[HONO_2]$ is inferred from the NOy measurement. $[H_2CO]$, $[HO_2NO_2]$, and $[O(^1D)]$ are calculated from steady-state relations. $[H_2O]$, [OH], $[NO_2]$, and [NO] are measured. [HONO] is calculated as described in the text.

Table II: Relative HO_x emission indices:

Concorde	Age (min.)	HOy/NOy	EI NOy (gNO_2/kg fuel)	EI HOy (gOH/kg fuel)
#3	16	0.045	23	0.35 ± 0.15
#4-5	19	0.051	10	0.2 ± 0.1
ER-2	8 - 14	0.035	3-5	0.06 ± 0.02

References and Notes

1. D. L. Albritton *et al.*, *The Atmospheric Effects of Stratospheric Aircraft: Interim Assessment Report of the NASA High-Speed Research Program*, NASA Ref. Publ. 1333 (1993).

2. World Meteorological Organization, *Scientific Assessment of Ozone Depletion: 1994*, WMO Global Ozone Research and Monitoring Project - Report No. 37 *Chapter 11: Subsonic and Supersonic Aircraft Emissions,* (WMO, Geneva, Switzerland, 1995).

3. D. W. Fahey *et al., Science,* (in press 1995).

4. H. Hoshizaki, L. B. Anderson, and R. J. Conti, in *Proceedings of the Second Conference on CIAP,* November 1972, Cambridge, MA (A. J. Broderick, Ed.), DOT-TSC-OST-73-4, (NTIS, Springfield, VA, 1973).

5. R. C. Miake-Lye *et al. J. of Aircraft* **30**, 467 (1993).

6. M. Y. Danilin, A. Ebel, H. Elbern, H. Petry, *J. Geophys. Res.* **99**, 18951 (1994).

7. D. K. Weisenstein, M. K. W. Ko, J. M. Rodriguez, N. -D. Sze, *Geophys. Res. Lett.* **18**, 1991 (1991).

8. J. M. Rodriguez *et al., Science* **261**, 1128 (1993) and references therein.

9. F. Arnold, J. Scheid, Th. Stilp, H. Schlager, M. E. Reinhardt, *Geophys. Res. Lett.*, **12**, 2421 (1992).

10. R. A. Cox and R. G. Derwent, *J. Photochem.* **6**, 23 (1976). Night-time losses may be dominated by heterogeneous loss of HONO on sulfate aerosols, see R. Zhang, M.-T. Leu, and L. F. Keyser, *J. Phys. Chem.* (submitted 1995).

11. $OH + SO_2$ is catalytic with respect to HOx: $OH + SO_2 + M \rightarrow HOSO_2$, followed by $HOSO_2 + O_2 \rightarrow HO_2 + SO_3$. SO_3 is converted to H_2SO_4 via reaction with water: $SO_3 + H_2O \rightarrow H_2SO_4$, see C. E. Kolb *et al., J. Am. Chem. Soc.* **116**, 10314 (1994).

12. P. O. Wennberg *et. al., Rev. Sci. Instr.* **65**, 1858 (1994).

13. P. O. Wennberg *et al., J. Atmos. Science.* (In press, 1995).

14. This observation requires that the source of OH in the plume must have a short lifetime. The photolysis of HONO, which has a short photochemical lifetime (τ = 6 min.), is consistent with this requirement. Other possible sources, such as formaldehyde (H_2CO), hydrogen peroxide (H_2O_2), and peroxynitric acid (HO_2NO_2), have photochemical lifetimes that are too long (5 hours, 1.25 days, and 1.5 days, respectively) and would not disappear in the time scale of the plume measurement.

15. R. C. Cohen *et al., Geophys. Res. Lett.* **21**, 2539 (1994).

16. NO_2 concentrations can be calculated from a steady state model or obtained from measurements (3). For concentrations inside the plume, we use the mean of the measured and steady state NO_2 values, and attribute an additional ±25% uncertainty to this concentration.

17. DeMore *et al., Jet Propul. Lab Publ.* 94-26 (1994).

18. R. J. Salawitch *et al., Geophys. Res. Lett.* **21**, 2547 (1994).

19. R. C. Miake-Lye *et al.,* in *The Atmospheric Effects of Stratospheric Aircraft: A Fourth Program Report*, NASA Ref. Publ. 1359 (1995).

20. M. R. Williams, in *Proceedings of the Second Conference on CIAP,* November 1972, Cambridge, MA (A. J. Broderick, Ed.), DOT-TSC-OST-73-4, (NTIS, Springfield, VA, 1973).

21. SPADE: The Stratospheric Photochemistry, Aerosols, and Dynamics Expedition. S. C. Wofsy, R. C. Cohen, A. L. Schmeltekopf, *Geophys. Res. Lett.* **21**, 2535 (1994).

22. D. W. Fahey *et al., J. Geophys. Res.* **100**, 3065 (1995).

23. J. Neely and D. L. Davidson in *Proceedings of the Second Conference on CIAP,* November 1972, Cambridge, MA (A. J. Broderick, Ed.), DOT-TSC-OST-73-4, (NTIS, Springfield, VA, 1973).

24. W. K. McGregor, B. L. Seiber, J. D. Few, *ibid.*

25. P. S. Zurer, *Chem. and Engin. News* **73**, 10 (1995).

Figure 1. A schematic of the evolution of HOx chemistry within the engine exhaust plume. The plume is separated into a HONO formation region, where OH is sequestered into HONO on a fast time scale, followed by a HONO photolysis region, where OH is produced on a slower time scale. Reactive hydrogen is emitted at the exit plane of the engine primarily as HOy (OH + HONO). Within seconds of emission most of the OH in the exhaust reacts with NO to form HONO. Only small amounts of OH react with emitted NO_2 and SO_2 to form $HONO_2$ and $HOSO_2$ (Eqs. 2-3) before HONO is formed. The majority of OH plume chemistry occurs on a much slower time scale, minutes after the emission. HONO is photolyzed, producing OH which reacts with NO_2 and SO_2. Eventually, most of the HOy emitted from the engine is converted to $HONO_2$.

Figure 2 OH (solid line) and HO_2 (broken line) mixing ratios measured during three crossings of the Concorde exhaust plume (a-c) and the single encounter with the ER-2 plume (d). The gaps in the data occur during background calibration of the OH flourescence signal and (in panel c) during a calibration of the chemical titration of HO_2. The encounters occurred at Greenwich times of (a) 10384 s, (b) 12697 s, (c) 12964 s, and (d) 15564 s. The plume ages are 16, 60, and 66 minutes for the Concorde exhaust and 10 minutes for the ER-2 exhaust. Meteorological conditions were: altitude 16.2 km, temperature 222 K, and pressure 100 mb. The Concorde plumes correspond to encounters 3, 9, and 11 observed by the NOy instrument (3).

Figure 3 (a) Time evolution of OH produced from HONO photolysis in the Concorde plume. The five measurements (solid circles) are scaled relative to the amount of NOy in each encounter. The error bars are the 2σ uncertainties of the measurements. The solid line is the result of the integrating model with HONO/NOy = 0.04. The dotted line corresponds to the 0.3 ppt background level of OH. Oxidation of (b) $NO_2 \rightarrow HNO_3$ and (c) $SO_2 \rightarrow SO_3$ in the plume is shown versus plume age. The oxidation ratio is the ratio of emitted NOy or SOx that is oxidized by emitted OH to the total NOx or SOx emitted from the engine. The solid line represents the oxidation ratio for HOy/NOy = 0.05. The shaded region includes the 1σ uncertainty of the calculation. The dashed line in (c) represents the oxidation ratio of SOx assuming all HOy is emitted as OH. The maximum of the shaded region in (c) includes this offset.